

Dynamically assisted pair production for scalar QED by two fields

Zi-Liang Li¹, Ding Lu¹, Bai-Song Xie^{1,2,†}

¹Key Laboratory of Beam Technology and Materials Modification of the Ministry of Education,
and College of Nuclear Science and Technology, Beijing Normal University, Beijing 100875, China

²Beijing Radiation Center, Beijing 100875, China

Corresponding author. E-mail: †bsxie@bnu.edu.cn

Received September 22, 2014; accepted November 20, 2014

By solving the quantum Vlasov equation, the dynamically assisted pair production for scalar quantum electrodynamics (QED) is investigated. It is verified that this mechanism still holds true for boson pair production. Two combinations of two electric fields having different time scales under various time delays are considered; it is found that the oscillations of the momentum spectrum and the number density of created bosons decrease with increasing time delay, and the latter has a maximum value when the time delay equals zero. Furthermore, the differences in vacuum pair production between bosons and fermions are also studied, and they are helpful for distinguishing the created bosons from fermions.

Keywords quantum Vlasov equation, dynamically assisted pair production, scalar QED

PACS numbers 12.20.Ds, 11.15.Tk, 02.60.Nm

1 Introduction

In relativistic quantum mechanics, the free electron solution of the Dirac equation involves an energy gap $2m_e$ consisting of negative- and positive-energy states. Further, the negative-energy problem is solved using the Dirac sea picture; i.e., the negative-energy states (Dirac sea) are filled with negative-energy electrons so that positive-energy electrons cannot dive into the Dirac sea. Therefore, the Dirac vacuum is stable in the absence of external influences. However, in the presence of a strong external electric field, the negative- and positive-energy levels will cross each other, and it is possible for an electron to be pulled out of the Dirac sea and remain as a hole there (explained as a positron) by quantum tunneling. This is a physical geometry of nonperturbative electron–positron pair production [1–5]. To observe this mechanism in the laboratory, the electric field strength should be comparable to that of the critical electric field, $E_{\text{cr}} = m_e^2/e \sim 1.3 \times 10^{16}$ V/cm, which corresponds to a laser intensity I_{cr} of $E_{\text{cr}}^2/(8\pi) \sim 2.3 \times 10^{29}$ W/cm² according to the Schwinger formula. Here m_e is the electron mass, and e is the magnitude of the electron charge. Natural units, $\hbar = c = 1$, are used in this paper. Another mechanism for overcoming the energy gap $2m_e$ and

producing electron–positron pairs is called perturbative multiphoton pair production. By absorbing a number of photons, the negative-energy electrons can jump directly into positive-energy states, leaving a hole in the Dirac sea.

The above two mechanisms are separated by the adiabatic Keldysh parameter $\gamma = m/|q|E\tau$ [6], $\gamma \ll 1$ for the nonperturbative process and $\gamma \gg 1$ for the perturbative process, where m and q are the particle mass and electric charge, respectively; E is the electric field strength, and τ is the time scale of the external field. Although perturbative multiphoton pair creation has been observed experimentally at the Stanford Linear Accelerator Center in the E-144 experiment [7], nonperturbative pair production is still a challenge experimentally because of the very high electric field strength required. To realize its detection, many works have reported theoretical analyses of nonperturbative pair production [8–19]. Further, many convenient numerical calculations of this non-Markovian process have been performed, for example, by solving the quantum Vlasov equation (QVE) [20–28].

In particular, the authors in Ref. [8] suggested the dynamically assisted Schwinger mechanism and found that the rate of pair creation could be significantly enhanced by using a combined electric field composed of electric fields with different time scales. This mechanism is ex-

pected to be used to detect electron–positron pair production from the vacuum for the first time by employing the ultrahigh-intensity laser pulses under development (e.g., the Extreme Light Infrastructure). However, does the dynamically assisted Schwinger mechanism still hold true for boson pair production? Though boson pair production requires a high field strength (for instance, the critical field strength for pion pair production is 273 times that for electron–positron pair creation), its off-equilibrium and nonperturbative signatures are valuable for understanding the pair production process in quantum chromodynamics [29, 30] as well as nonperturbative phenomena in atomic molecular physics. In studying the momentum spectra of created pairs, it is also helpful to distinguish boson pair production from fermion pair creation in complex background events. Furthermore, it is also simple to use scalar QED to interpret novel phenomena occurring in pair production in terms of a quantum mechanical scattering picture.

In this study, we generalize the dynamically assisted Schwinger mechanism to boson pair creation by solving the QVE, which can yield both the momentum spectra and number density of created pairs. In particular, we consider the boson pair production for two combined electric fields, each composed of two electric fields with different time scales and either the same or opposite signs. The effect of the time delay between the strong and weak electric fields on pair creation is also studied. Moreover, we present the differences in pair production between bosons and fermions, which can be used to distinguish boson pair production from fermion pair creation.

2 Quantum Vlasov equation

Our starting point is the Boltzmann equation describing the time evolution of the single-particle distribution function $f(\mathbf{x}, \mathbf{k}, t)$, $df/dt = \mathcal{C} + \mathcal{S}$, where \mathcal{C} is the collision term, and \mathcal{S} denotes a source term related to pair production. Here we consider the field at an antinode of the standing wave field formed by two counterpropagating laser pulses and focus on the region where the magnetic field can be neglected. Therefore, the magnetic field effects are not considered. Furthermore, because the laser spatial focusing scales are much larger than the spatial scales of pair production, the spatial effects are also neglected. Consequently, we have a spatially homogeneous time-varying electric field. For this field $\mathbf{E}(t) = (0, 0, E(t))$, which corresponds to a vector potential $\mathbf{A}(t) = (0, 0, A(t))$ with $E(t) = -\dot{A}(t)$, the source term for scalar QED was

derived in Ref. [21]: $\mathcal{S} = (Q(\mathbf{k}, t)/2) \int_{t_0}^t dt' Q(\mathbf{k}, t') [1 + 2f(\mathbf{k}, t')] \cos[2\Theta(\mathbf{k}, t', t)]$. Here t' is the integral variable representing the change from the initial time t_0 to the time t ; $\mathbf{k} = (\mathbf{k}_\perp, k_{\parallel})$ is the canonical momentum; $Q(\mathbf{k}, t) = qE(t)k_{\parallel}(t)/\omega^2(\mathbf{k}, t)$ represents the amplitude of the pair creation excitation, which describes the ability to create bosons; and $\Theta(\mathbf{k}, t', t) = \int_{t'}^t d\tau \omega(\mathbf{k}, \tau)$ denotes the high-frequency phase, which may lead to interference effects. Further, q is the boson charge, $k_{\parallel}(t) = k_{\parallel} - eA(t)$ is the kinetic momentum along the electric field $E(t)$, and $\omega(\mathbf{k}, t) = \sqrt{\varepsilon_\perp^2 + k_{\parallel}^2(t)}$ is the total energy of created particles with the transverse energy $\varepsilon_\perp = \sqrt{m^2 + \mathbf{k}_\perp^2}$ and boson mass m .

In a subcritical electric field $E \lesssim 0.1E_{\text{cr}}$, the particle number created from the vacuum is very small; thus, the effect of collisions can be ignored. Finally, we can obtain the following integro-differential equation for the single-particle momentum distribution function $f(\mathbf{k}, t)$ (QVE):

$$\frac{df(\mathbf{k}, t)}{dt} = \frac{1}{2} \frac{qE(t)k_{\parallel}(t)}{\omega^2(\mathbf{k}, t)} \int_{t_0}^t dt' \frac{qE(t')k_{\parallel}(t')}{\omega^2(\mathbf{k}, t')} \times [1 + 2f(\mathbf{k}, t')] \cos \left[2 \int_{t'}^t d\tau \omega(\mathbf{k}, \tau) \right]. \quad (1)$$

One can find that the high-frequency phase also reflects the non-Markovian process of pair creation because it depends on the history of the external electric field. Furthermore, the factor in the first integral, $1 + 2f(\mathbf{k}, t')$, reflects both the non-Markovian process of pair creation and the effect of quantum statistics on boson pair production. It is also called the Bose enhancement factor, as each momentum state allows more than one pair of bosons. We emphasize that only when the external electric field becomes zero at $t \rightarrow +\infty$ does the distribution function $f(\mathbf{k}, t)$ describe the real particles created from vacuum. Thus, the important quantities are the momentum distribution function $f(\mathbf{k}, +\infty)$ and the particle number density $n(+\infty)$. Eq. (1) can also describe fermion pair production if $k_{\parallel}(t)$ is replaced with ε_\perp and the Bose enhancement factor is replaced with a Pauli blocking factor $1 - 2f(\mathbf{k}, t')$.

By introducing two auxiliary quantities,

$$u(\mathbf{k}, t) = \int_{t_0}^t dt' Q(\mathbf{k}, t') [1 + 2f(\mathbf{k}, t')] \cos[2\Theta(\mathbf{k}, t', t)], \quad (2)$$

$$v(\mathbf{k}, t) = \int_{t_0}^t dt' Q(\mathbf{k}, t') [1 + 2f(\mathbf{k}, t')] \sin[2\Theta(\mathbf{k}, t', t)], \quad (3)$$

Eq. (1) can be equivalently transformed into a first-order ordinary differential equation system:

$$\dot{f}(\mathbf{k}, t)dt = \frac{1}{2}Q(\mathbf{k}, t)u(\mathbf{k}, t), \tag{4}$$

$$\dot{u}(\mathbf{k}, t)dt = Q(\mathbf{k}, t)[1 + 2f(\mathbf{k}, t)] - 2\omega(\mathbf{k}, t)v(\mathbf{k}, t), \tag{5}$$

$$\dot{v}(\mathbf{k}, t)dt = 2\omega(\mathbf{k}, t)u(\mathbf{k}, t), \tag{6}$$

where the dot denotes the total time derivative.

Finally, using the initial conditions $f(\mathbf{k}, -\infty) = u(\mathbf{k}, -\infty) = v(\mathbf{k}, -\infty) = 0$, one can obtain the single-particle momentum distribution function $f(\mathbf{k}, t)$ by numerically solving Eqs. (4)–(6). Then the number density of created bosons can be obtained by integrating $f(\mathbf{k}, +\infty)$ over the momentum as

$$n(+\infty) = \int \frac{d^3k}{(2\pi)^3} f(\mathbf{k}, +\infty). \tag{7}$$

For fermion pair production, a degeneracy factor 2 appears before the right-hand side of Eq. (7).

3 Results

To numerically solve the QVE, the electric field strength is normalized by the critical field strength $E_{cr} = m^2/q$, and the other quantities are normalized by the particle mass m or $1/m$. We first discuss the roles of the charge and mass of created particles in pair production. According to our normalization, it can be seen that their effects on pair production are exhibited from the electric field strength E as $q \propto E$ and $m \propto 1/\sqrt{E}$. The variations in the distribution function with the particle charge and mass are plotted in Fig. 1(a) and (b), respectively. The pair yield grows with increasing particle charge but decreases with increasing particle mass. This indicates that to create a pair of massive particles, a stronger electric field is needed. Because the effects of the charge and mass of the created particles on the dynamically assisted pair production are contained in the effect of the electric field strength, we set $q = m = 1$ and $\mathbf{k}_\perp = 0$ for convenience.

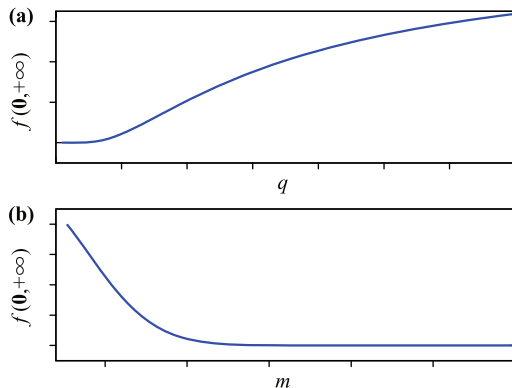


Fig. 1 Sketches of the distribution function $f(\mathbf{0}, +\infty)$ as a function of (a) the particle charge q , and (b) the particle mass m .

Reference [8] reports that the superposition of a strong but slowly varying electric field with a weak but rapidly changing one significantly enhances the vacuum electron–positron pair production. This can be intuitively interpreted as the dynamic assistance effect of the perturbative multiphoton mechanism on nonperturbative Schwinger pair production. To study this effect for boson pair production, we consider two different combinations of a strong, long-pulse electric field $E_1(t)$ and a weak, short-pulse field $E_2(t)$ with different time delays.

The first type of combined electric field is described by

$$E_A(t) = E_1(t) + E_2(t) = E_1 \text{sech}^2\left[\omega_1\left(t + \frac{T}{2}\right)\right] + E_2 \text{sech}^2\left[\omega_2\left(t - \frac{T}{2}\right)\right], \tag{8}$$

where E_1 and E_2 are the electric field amplitudes, ω_1 and ω_2 are the inverse pulse widths of the electric fields, and T denotes the time delay between $E_1(t)$ and $E_2(t)$. The following electric field parameters are chosen: $E_1 = 0.25$, $\omega_1 = 0.02$, and $E_2 = 0.025$, $\omega_2 = 1$. It can be seen that the Keldysh parameter for the strong electric field is $\gamma_1 = \omega_1/E_1 = 0.08 \ll 1$, which belongs to the nonperturbative regime, and that for the weak field is $\gamma_2 = \omega_2/E_2 = 40 \gg 1$, which belongs to the perturbative regime. However, neither Keldysh parameter, γ_1 nor γ_2 , can totally describe the results of dynamically assisted pair production for the combined electric fields. Therefore, we introduce the combined Keldysh parameter $\gamma = \omega_2/E_1$ [8, 16] to study the enhanced pair production.

When the time delay $T = 0$, the combined electric field $E_A(t)$ is symmetric and has a maximum value $E_1 + E_2$ at the time $t = 0$. The longitudinal momentum spectrum of created bosons in this case, obtained by numerically solving Eq. (1), is shown as a dashed blue line in Fig. 2(a). It can be seen that dynamically assisted pair production is still valid for boson pair creation (see also Fig. 4), and oscillatory structures in the momentum spectrum also appear. Furthermore, the momentum spectrum of bosons is compared with that of fermions (solid red line). Clearly, the enhancement of pair creation for bosons is weaker than that for fermions, and the oscillation speed for bosons is slightly slower than that for fermions.

The longitudinal momentum spectra of the created bosons for various time delays T are presented in Fig. 3 for a time delay $T \neq 0$. The following values of T are chosen: 10 (green line), 20 (blue line), 30 (cyan line), 40 (magenta line), 50 (olive line), and 80 (navy line). For reference, the momentum spectrum of created bosons in a strong but slowly varying electric field $E_1(t)$ (dashed red line) is also plotted. The oscillation behaviors be-

come weaker with increasing time delay. In particular, when $T \gtrsim 80$, the oscillations almost disappear, and the momentum distributions for the electric fields $E_1(t)$ and $E_2(t)$ are well separated. Further, dynamically assisted pair production is no longer obvious (see Fig. 4). With increasing $|T|$, the number density of created bosons for the combined electric field $E_A(t)$ decreases and finally equals the sum of the particle number densities for the electric fields $E_1(t)$ and $E_2(t)$. Therefore, to increase the probability of pair production, it is necessary to shorten the time delay between these two electric fields. Moreover, one can find that when the longitudinal momentum $k_{//} > 0$, the momentum spectrum for the combined electric field $E_A(t)$ and that for the electric field $E_1(t)$ almost overlap. However, small differences still appear between them because the created bosons in the electric field $E_1(t)$ will be accelerated by the electric field $E_2(t)$. This result is similar to that for fermion pair production in Ref. [16].

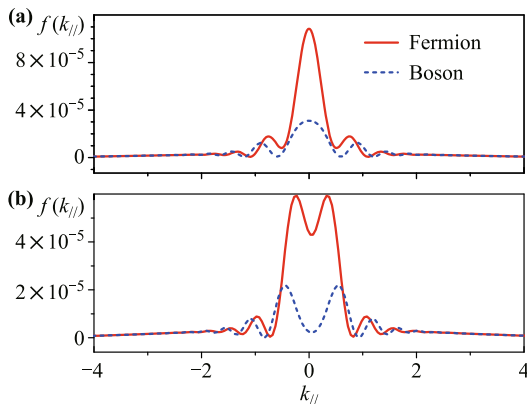


Fig. 2 The longitudinal momentum spectrum of created bosons (dashed blue line) and fermions (solid red line) for (a) the combination of same-sign electric fields, $E_A(t)$, and (b) the combination of opposite-sign electric fields, $E_B(t)$. The electric field parameters are $E_1 = 0.25$, $\omega_1 = 0.02$, and $E_2 = 0.025$, $\omega_2 = 1$ with the time delay $T = 0$.

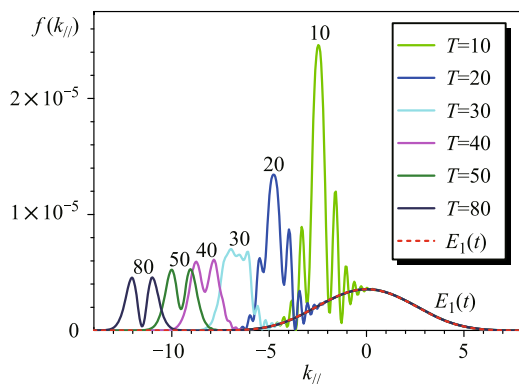


Fig. 3 The longitudinal momentum spectrum of created bosons changing with the time delay T for the combination of same-sign electric fields, $E_A(t)$. The electric field parameters are $E_1 = 0.25$, $\omega_1 = 0.02$, and $E_2 = 0.025$, $\omega_2 = 1$.

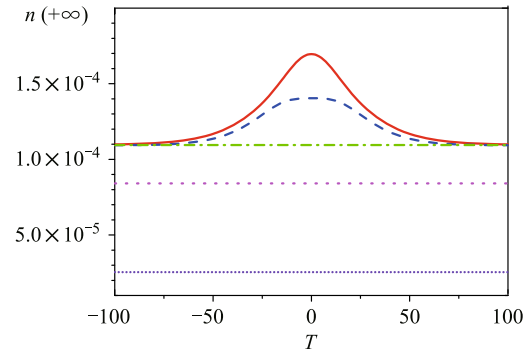


Fig. 4 The number density of created bosons $n(+\infty)$ as a function of the time delay T for the combination of same-sign electric fields, $E_A(t)$ (solid red line), the combination of opposite-sign electric fields, $E_B(t)$ (dashed blue line), the strong but slowly varying electric field $E_1(t)$ (dotted magenta line), and the weak but rapidly changing electric field $\pm E_2(t)$ (short dotted violet line). The dash-dotted green line denotes the sum of the produced particle number density for $E_1(t)$ and $\pm E_2(t)$. The electric field parameters are $E_1 = 0.25$, $\omega_1 = 0.02$, and $E_2 = 0.025$, $\omega_2 = 1$.

Next, we consider the second type of combined electric field composed of the strong but slowly varying electric field $E_1(t)$ minus the weak but rapidly changing one $E_2(t)$,

$$E_B(t) = E_1(t) - E_2(t) = E_1 \text{sech}^2 \left[\omega_1 \left(t + \frac{T}{2} \right) \right] - E_2 \text{sech}^2 \left[\omega_2 \left(t - \frac{T}{2} \right) \right]. \quad (9)$$

The parameters are the same as those for the first combined electric field.

When the time delay T is 0, the combined electric field $E_B(t)$ is also symmetric and has a local minimal value $E_1 - E_2$ at the time $t = 0$. The longitudinal momentum spectrum of produced bosons (dashed blue line) in this situation was calculated and is plotted in Fig. 2(b). There are two noticeable differences between the momentum spectra in Figs. 2(a) and (b). First, the momentum distribution function $f(k_{//})$ is smaller than that for the combination of same-sign electric fields, $E_A(t)$; this is because the strong but slowly varying electric field $E_1(t)$ is weakened by the weak but rapidly changing one $E_2(t)$. Second, for a small longitudinal momentum $k_{//}$, the single-hump structure of the momentum spectrum in Fig. 2(a) is replaced by a double-hump one. Moreover, dynamically assisted pair production still occurs for the combination of opposite-sign electric fields, $E_B(t)$ (dashed blue line; see Fig. 4).

When the time delay $T \neq 0$, the longitudinal momentum spectra of created bosons for various T values are shown in Fig. 5. The variation trend is similar to that of the first combined electric field, $E_A(t)$. Nevertheless, dynamically assisted pair production is always weaker than that for $E_A(t)$, and a flat-topped region appears in the

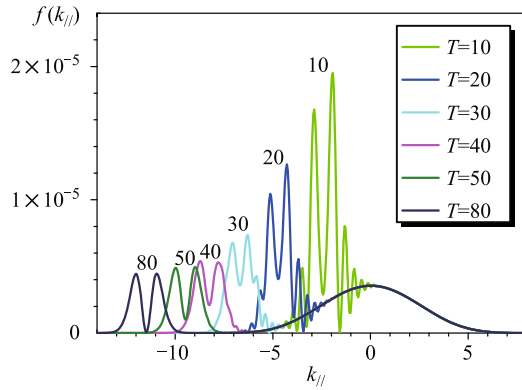


Fig. 5 The longitudinal momentum spectrum of created bosons changing with the time delay T for the combination of opposite-sign electric fields, $E_B(t)$. The electric field parameters are $E_1 = 0.25$, $\omega_1 = 0.02$, and $E_2 = 0.025$, $\omega_2 = 1$.

particle number density $n(+\infty)$. It indicates that, in this region, dynamically assisted pair production is insensitive to the time delay, whereas beyond this region, the particle number density will decrease rapidly with time delay $|T|$. In particular, when $|T| \rightarrow 100$, dynamically assisted pair production will completely vanish because the electric fields $E_1(t)$ and $E_2(t)$ are completely separate.

Now we study the enhancement of the number density of created pairs in dynamically assisted pair production using more reasonable electric field parameters that can be achieved in upcoming experiments. The results are plotted in Fig. 6 for the combined electric field $E_A(t)$. Here, $n_{1+2}/(n_1+n_2)$ is the ratio between the particle number density for $E_A(t)$ and the sum of the number densities for $E_1(t)$ and $E_2(t)$. The created pair yield can be greatly enhanced by superimposing a weak short-duration electric field on a strong long-duration one. Further, for a small combined Keldysh parameter γ , the nonperturbative mechanism plays an important role in pair creation, and the perturbative process is not significant. In this region, the enhancement is realized by simply increasing the strength of the strong electric field. For large γ , the perturbative process dominates pair production, and the nonperturbative mechanism can be neglected; thus, the enhancement fades with increasing combined Keldysh parameter. However, when nonperturbative pair production is comparable to the perturbative process, the number density of created particles can be immensely enhanced; see the pronounced enhancement peaks in Fig. 6. This is due to the resonance effect between nonperturbative pair production and the perturbative process. Intuitively, when these two mechanisms are comparable to each other, the strong electric field can more easily lower the threshold of multiphoton pair creation, while the rapidly changing electric field will provide additional channels for nonperturbative pair production. Moreover,

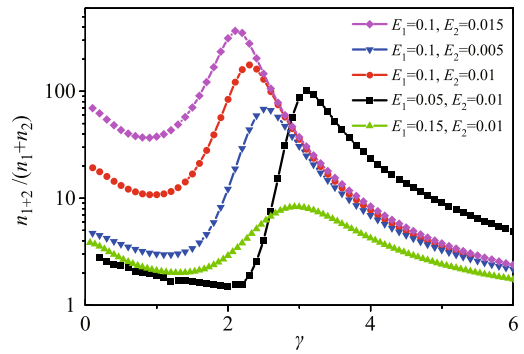


Fig. 6 Enhancement of the number density in dynamically assisted pair production for the combined electric field $E_A(t)$. We fix $\omega_1 = 0.01$ and change γ or, equivalently, change ω_2 .

for different electric field parameters, the enhancement peaks are not fixed but change at $\gamma \sim \mathcal{O}(1)$. The above results are valuable for clarifying pair creation in quantum chromodynamics, such as the two-photon production of pion pairs [29, 30]. Additionally, in this nonperturbative multiphoton region, because pair production includes both nonperturbative and perturbative processes, there will be many novel phenomena that are worthy of further study in the future.

5 Summary and discussion

In summary, this paper investigates dynamically assisted pair production for scalar QED by solving the QVE. It is verified that this mechanism still holds true for boson pair creation from vacuum. The longitudinal momentum spectrum and number density of created bosons for various time delays T are studied for a combination of same-sign electric fields and a combination of opposite-sign electric fields. Boson pair production is found to decrease with increasing time delay $|T|$ and have a maximum value at $T = 0$ for these two combined electric fields. Moreover, the differences between the longitudinal momentum spectra of bosons and fermions for dynamically assisted pair production are also studied. Physically, the differences are related to the different spins of bosons and fermions. Our results are expected to deepen the understanding of dynamically assisted pair production in terms of scalar QED. They are applicable to an optimal theory for detecting pair production in the laboratory. Furthermore, it is useful to understand nonperturbative pair production phenomena in particle physics and atomic molecular physics.

In addition, although the oscillatory structure of the momentum spectrum is presented for dynamically assisted pair production, it differs from the interference effect found in Refs. [14, 15, 17]. This is because there is

only one pair of semiclassical turning points dominating pair production. Thus, the underlying physical reason for this oscillation still needs further study in the future.

Acknowledgements This work was supported by the National Natural Science Foundation of China (NSFC) (Grant Nos. 11475026 and 11335013) and partially by the Open Fund of National Laboratory of Science and Technology on Computational Physics at IAPCM and the Fundamental Research Funds for the Central Universities (FRFCU).

References

1. F. Sauter, Über das Verhalten eines elektrons im homogenen elektrischen feld nach der relativistischen theorie Diracs, *Z. Phys.* 69(11–12), 742 (1931)
2. W. Heisenberg and H. Euler, Folgerungen aus der Diracschen theorie des positrons, *Z. Phys.* 98(11–12), 714 (1936)
3. J. Schwinger, On gauge invariance and vacuum polarization, *Phys. Rev.* 82(5), 664 (1951)
4. A. I. Nikishov, Barrier scattering in field theory removal of Klein paradox, *Nucl. Phys. B* 21(2), 346 (1970)
5. V. S. Popov, *Sov. Phys. JETP* 35, 659 (1972)
6. L. V. Keldysh, *Sov. Phys. JETP* 20, 1018 (1965)
7. D. L. Burke, R. Field, G. Horton-Smith, J. Spencer, D. Walz, S. Berridge, W. Bugg, K. Shmakov, A. Weidemann, C. Bula, K. McDonald, E. Prebys, C. Bamber, S. Boege, T. Koffas, T. Kotseroglou, A. Melissinos, D. Meyerhofer, D. Reis, and W. Ragg, Positron production in multiphoton light-by-light scattering, *Phys. Rev. Lett.* 79(9), 1626 (1997)
8. R. Schützhold, H. Gies, and G. Dunne, Dynamically assisted Schwinger mechanism, *Phys. Rev. Lett.* 101(13), 130404 (2008)
9. G. V. Dunne, New strong-field QED effects at extreme light infrastructure, *Eur. Phys. J. D* 55(2), 327 (2009)
10. D. B. Blaschke, A. V. Prozorkevich, G. Röpke, C. D. Roberts, S. M. Schmidt, D. S. Shkirmanov, and S. A. Smolyansky, Dynamical Schwinger effect and high-intensity lasers: Realising nonperturbative QED, *Eur. Phys. J. D* 55(2), 341 (2009)
11. A. Di Piazza, E. Lotstedt, A. I. Milstein, and C. H. Keitel, Barrier control in tunneling e^+e^- photoproduction, *Phys. Rev. Lett.* 103(17), 170403 (2009)
12. G. V. Dunne, H. Gies, and R. Schützhold, Catalysis of Schwinger vacuum pair production, *Phys. Rev. D* 80(11), 111301 (2009)
13. S. S. Bulanov, V. D. Mur, N. B. Narozhny, J. Nees, and V. S. Popov, Multiple colliding electromagnetic pulses: A way to lower the threshold of e^+e^- pair production from vacuum, *Phys. Rev. Lett.* 104(22), 220404 (2010)
14. C. K. Dumlu and G. V. Dunne, Stokes phenomenon and Schwinger vacuum pair production in time-dependent laser pulses, *Phys. Rev. Lett.* 104(25), 250402 (2010)
15. C. K. Dumlu and G. V. Dunne, Interference effects in Schwinger vacuum pair production for time-dependent laser pulses, *Phys. Rev. D* 83(6), 065028 (2011)
16. M. Orthaber, F. Hebenstreit, and R. Alkofer, Momentum spectra for dynamically assisted Schwinger pair production, *Phys. Lett. B* 698(1), 80 (2011)
17. E. Akkermans and G. V. Dunne, Ramsey fringes and time-domain multiple-slit interference from vacuum, *Phys. Rev. Lett.* 108(3), 030401 (2012)
18. C. Fey and R. Schützhold, Momentum dependence in the dynamically assisted Sauter–Schwinger effect, *Phys. Rev. D* 85(2), 025004 (2012)
19. Z. L. Li, D. Lu, and B. S. Xie, Multiple-slit interference effect in the time domain for boson pair production, *Phys. Rev. D* 89(6), 067701 (2014)
20. Y. Kluger, E. Mottola, and J. M. Eisenberg, Quantum Vlasov equation and its Markov limit, *Phys. Rev. D* 58(12), 125015 (1998)
21. S. Schmidt, D. Blaschke, G. Röpke, S. A. Smolyansky, A. V. Prozorkevich, and V. D. Toneev, A quantum kinetic equation for particle production in the Schwinger mechanism, *Int. J. Mod. Phys. E* 07(06), 709 (1998)
22. R. Alkofer, M. B. Hecht, C. D. Roberts, S. M. Schmidt, and D. V. Vinnik, Pair creation and an X-ray free electron laser, *Phys. Rev. Lett.* 87(19), 193902 (2001)
23. C. D. Roberts, S. M. Schmidt, and D. V. Vinnik, Quantum effects with an X-ray free-electron laser, *Phys. Rev. Lett.* 89(15), 153901 (2002)
24. D. B. Blaschke, A. V. Prozorkevich, C. D. Roberts, S. M. Schmidt, and S. A. Smolyansky, Pair production and optical lasers, *Phys. Rev. Lett.* 96(14), 140402 (2006)
25. A. Nuriman, B. S. Xie, Z. L. Li, and D. Sayipjamal, Enhanced electron–positron pair creation by dynamically assisted combinational fields, *Phys. Lett. B* 717(4–5), 465 (2012)
26. N. Abdurkerim, Z. L. Li, and B. S. Xie, Effects of laser pulse shape and carrier envelope phase on pair production, *Phys. Lett. B* 726(4–5), 820 (2013)
27. Z. L. Li, D. Lu, B. S. Xie, L. B. Fu, J. Liu, and B. F. Shen, Enhanced pair production in strong fields by multiple-slit interference effect with dynamically assisted Schwinger mechanism, *Phys. Rev. D* 89(9), 093011 (2014)
28. O. Oluk, B. S. Xie, M. A. Bake, and S. Dulat, Electron-positron pair production in a strong asymmetric laser electric field. *Phys.* 9(2), 157 (2014)
29. J. Boyer, F. Butler, G. Gidal, G. Abrams, D. Amidei, et al., Two-photon production of pion pairs, *Phys. Rev. D* 42(5), 1350 (1990)
30. J. Dominick, M. Lambrecht, S. Sanghera, V. Shelkov, T. Skwarnicki, et al., Two-photon production of charged pion and kaon pairs, *Phys. Rev. D* 50(5), 3027 (1994)